econometrics

MDPI

Article

Volatility Analysis of Returns of Financial Assets Using a Bayesian Time-Varying Realized GARCH-Itô Model

Pathairat Pastpipatkul and Htwe Ko *

Faculty of Economics, Chiang Mai University, Chiang Mai 50200, Thailand; pathairat.past@cmu.ac.th
* Correspondence: pdohtweko@gmail.com

Abstract

In a stage of more and more complex and high-frequency financial markets, the volatility analysis is a cornerstone of modern financial econometrics with practical applications in portfolio optimization, derivative pricing, and systematic risk assessment. This paper introduces a novel Bayesian Time-varying Generalized Autoregressive Conditional Heteroskedasticity (BtvGARCH-Itô) model designed to improve the precision and flexibility of volatility modeling in financial markets. Original GARCH-Itô models, while effective in capturing realized volatility and intraday patterns, rely on fixed or constant parameters; thus, it is limited to studying structural changes. Our proposed model addresses this restraint by integrating the continuous-time Ito process with a time-varying Bayesian inference to allow parameters to vary over time based on prior beliefs to quantify uncertainty and minimize overfitting, especially in small-sample or high-dimensional settings. Through simulation studies, using sample sizes of $N = 100$ and $N = 200$, we find that BtvGARCH-Itô outperformed original GARCH-Itô in-sample fit and out-of-sample forecast accuracy based on posterior estimates comparison with true parameter values and forecasting error metrics. For the empirical validation, this model is applied to analyze the volatility of S&P 500 and Bitcoin (BTC) using one-minute length data for S&P 500 (from 3 January 2023 to 31 December 2024) and BTC (from 1 January 2023 to 1 January 2025). This model has potential as a robust tool and a new direction in volatility modeling for financial risk management.

Keywords: volatility analysis; S&P 500; BTC; BtvGARCH-Itô

Academic Editor: Deborah Gefang

Received: 18 July 2025
Revised: 29 August 2025
Accepted: 1 September 2025
Published: 9 September 2025

Citation: Pastpipatkul, P., & Ko, H. (2025). Volatility Analysis of Returns of Financial Assets Using a Bayesian Time-Varying Realized GARCH-Itô Model. *Econometrics*, *13*(3), 34. https://doi.org/10.3390/econometrics13030034

1. Introduction

Modeling financial asset volatility is very important for option pricing, managing risk, and building investment portfolios (Opschoor & Lucas, 2023; Engle & Gallo, 2006). GARCH models, introduced by Engle (1982) and Bollerslev (1986), are commonly used to track how volatility changes over time. These models use daily squared returns to estimate volatility. However, they rely on limited information, which makes them less effective in catching market behavior. Fan and Wang (2007) argued that high-frequency financial data has improved how we measure volatility and forecasting performance. New measures like realized variance, bipower variation, realized kernel, intraday range, and multipower variation that use detailed intraday returns are found in the existing literature, including Barndorff-Nielsen and Shephard (2004), Barndorff-Nielsen et al. (2008), Todorov (2009), Carr and Wu (2003), and Huang and Tauchen (2005). These measures produce less biased estimates of volatility under the right conditions (Andersen et al., 2007).

Realized Generalized Autoregressive Conditional Heteroskedasticity (GARCH) models (Song et al., 2020; Kim & Wang, 2016) have built on these improvements. They model

both returns and realized volatility together. One key part of these models is the measurement equation, which links realized volatility directly to the model's estimate of true volatility. This setup improves performance compared to traditional GARCH models, for example, Song et al. (2020) account for both price jumps and volatilities. Realized GARCH-Itô models include more detailed data like integrated volatility and jump variation, and they help the models capture unexpected changes in prices. Realized GARCH-Itô models predict volatility better than earlier models (Kim & Wang, 2016), accounting for intraday U-shape volatility.

While significant progress has been made, these models assume constant and fixed parameters. This is a problem because financial markets are dynamic and change significantly over time. The concept of time-varying coefficients has been increasingly accepted in econometric models to help deal with this sort of issue. They let parameters adjust to varying market conditions and improve predictions during uncertain periods of structural changes, economic shocks, or even policy shifts. In fact, financial markets are constantly changing. Time-varying models also identify shifts in market dynamics and correlations (Andersen & Bollerslev, 1997; Andersen et al., 2019; Opschoor & Lucas, 2023). For example, time-varying GARCH coefficients show how the second-order dynamics of the U.S. stock market changed sharply after 2001 the internet bubble burst, while the Chinese market remained isolated (Gao et al., 2024). These models are effective in volatility predictions of future return distributions and risk measures. Moreover, they can handle non-stationarity, which is common in financial data.

In addition to time-varying models, Bayesian models treat all uncertainty as probability based on prior beliefs about how parameters might change over time. Furthermore, Bayesian inference estimates are all unknown parameters, while also showing how they might relate to each other. They are also beneficial when dealing with small datasets and even prevent overparameterization in high-dimensional settings. The combination of Bayesian inference to time-varying parameter models resulted in efficient posterior and improved forecasting accuracy (Koop & Korobilis, 2022; Taspinar et al., 2021; Kalli & Griffin, 2014; Jacquier et al., 2004). Using Bayesian methods together with time-varying parameters provides the effectiveness of modeling and volatility forecasting.

Given the importance and the need to adapt to continuously changing financial markets, this paper introduces a Bayesian Time-varying Realized GARCH-Itô (BtvGARCH-Itô) model. This model lets parameters vary over time, fits high-frequency data more effectively, and reduces uncertainty by using prior knowledge to improve the accuracy of volatility analysis in financial markets. For the empirical study, we apply the model to two contrasting assets: the S&P 500 index, representing a liquid and diversified equity market, and Bitcoin (BTC), a speculative digital asset with heavy tails and frequent jumps. These applications demonstrate the model's practical relevance and its superior performance compared to conventional GARCH-type models in modeling financial market volatility.

2. Realized GARCH-Itô Model

The realized GARCH-Itô model, first introduced by Song et al. (2020), presents a significant advancement in volatility analysis by integrating high-frequency financial data with continuous-time jump-diffusion processes. This hybrid model extends the united GARCH-Itô framework of Kim and Wang (2016) by incorporating realized volatility (RV) and jump variation (JV) as innovations. Thereby, Song et al. (2020) filled the gap between discrete-time econometric models and continuous-time stochastic processes. It is particularly effective to account for dynamic changes of volatility in financial markets, including high-frequency data analysis, whereas market noises, price jumps, and intraday

volatility patterns exist. The realized GARCH-Itô model is formulated as a stochastic differential equation. The log stock price process X_t for $t \epsilon R_+$ is as follows:

$$dX_t = \mu_t dt + \sigma_t(\theta) dB_t + L_t d\Lambda_t \quad (1)$$

where μ_t is the drift, $\sigma_t(\theta)$ is the instantaneous volatility, B_t is a Brownian motion, L_t is jump sizes, and Λ_t is a counting process for jumps. At integer times n, the conditional variance is:

$$\sigma_n^2(\theta) = \omega + \gamma\sigma_{n-1}^2(\theta) + \alpha \int_{n-1}^{n} \sigma_s^2(\theta) ds + \beta \int_{n-1}^{n} L_s^2 d\Lambda_s \quad (2)$$

where $\theta = (\omega, \alpha, \beta, \gamma)$, $\int_{n-1}^{n} \sigma_s^2(\theta) ds \approx RV_n$, $\int_{n-1}^{n} L_s^2 d\Lambda_s \approx JV_n$, and the integrated volatility over [n − 1, n] is:

$$\int_{[n-1]}^{n} \sigma_t^2(\theta) dt = h_n(\theta) + D_n \quad (3)$$

With

$$h_t(\theta) = \omega^g + \gamma h_{t-1}(\theta) + \alpha^g . RV_{t-1} + \beta^g JV_{t-1} \quad (4)$$

where h_t is the latent conditional variance at time t, ω^g is the baseline volatility, α^g is lagged realized volatility (RV_{t-1}), β^g is lagged jump variation (JV_{t-1}), γ is lagged variance of latent volatility, and θ = (ω^g, α^g, β^g, γ) parameters are assumed constant over time following a normal distribution.

The quasi-likelihood function used for the static parameters in this model is stated as:

$$\hat{L}_{n,m}^{GH}(\theta) = -\sum_{i=1}^{n} \left[log\left(\hat{h}_i(\theta)\right) + \frac{RV_i}{\hat{h}_i(\theta)} \right] \quad (5)$$

where $\hat{h}_i(\theta) = \sum_{l=1}^{i=1} \gamma^{i-1}\omega^g + \alpha^g RV_{i-l} + \beta^g JV_{i-l} + \gamma^{i-1} h_1(\theta)$, and $h_1(\theta) = \frac{\omega^g + \beta^g + \lambda_{\omega,L}}{1-\alpha^g-\gamma}$ subject to $\alpha^g + \gamma < 1$.

3. Bayesian Time-Varying GARCH-Itô Model

The Bayesian Time-varying GARCH-Itô (BtvGARCH-Itô) model extends the Generalized unified GARCH-Itô model by incorporating time-varying parameters and Bayesian inference to study dynamic volatility in high-frequency financial markets. This section delivers the BtvGARCH-Itô model specification, which is used to effectively estimate the latent volatility and its time-varying components using observed realized volatility, jump variation impact, and lagged variance within a Bayesian inference framework. This model is suitable for financial applications of high-frequency data analysis where volatility dynamics swing continuously. Thus, the BtvGARCH-Itô model is designed to account for the dynamic nature of financial market volatility. High-frequency returns reflect intraday price movements and rapid responses to market information. Time-varying coefficients allow the model to adjust to changing conditions, including structural shifts, monetary policy interventions, and speculative cycles. The latent volatility component (h_t) represents market risk, while the jump variation accounts for sudden price shocks, heavy tails, and extreme events common in both regulated equity markets like the S&P 500 and decentralized speculative markets like Bitcoin. The parameters ω (baseline volatility), α (realized volatility), β (jumps variation), and γ (latent volatility) are specified to reflect these features. The BtvGARCH-Itô model defines the latent volatility process $\{h_t\}_{t=1}^{N}$ as follows:

For t = 1

$$h_1 = \frac{\omega_1 + \beta_1 \lambda_{\omega,\, L}}{max(e,\, 1 - \alpha_1 - \gamma_1)},\ for\ small\ e > 0 \quad (6)$$

where $e > 0$ is a small constant ensuring positivity, and $\lambda_{\omega,\,L}$ is a constant derived from the empirical distribution of jump variation JV_t.

For t = 2, . . ., N

$$h_1 = \omega_t + \alpha_t RV_{t-1} + \beta_t JV_{t-1} + \gamma_t h_{t-1},\ for\ \mathrm{t} = 2, \ldots, \mathrm{N} \tag{7}$$

where RV_t is the realized volatility, JV_t is the jump variation, and $\omega_t^g,\ \alpha_t^g,\ \beta_t^g, \gamma_t \in (0,\ 1)$ are time-varying parameters satisfying $\alpha_t + \gamma_t < 1$..

The time-varying parameters shift via a Gaussian random walk in logit space:

$$\theta_t^{raw} = \theta_{t-1}^{raw} + \sigma_\theta \acute{\theta}_t,\ \theta_t = inv_{logit(\theta_t^{raw})} = \frac{1}{1 + exp(-\theta_t^{raw})} \tag{8}$$

where $\theta \in \{\omega, \alpha, \beta, \gamma\}$, and $\overset{\sim}{\theta}_t \sim N(0,1)$. The measurement equation is:

$$RV_t \sim N\left(h_t, \sigma_{RV}^2\right),\ \sigma_{RV} > 0 \tag{9}$$

To complete the Bayesian specification, we assign prior distributions as follows:

Initial coefficients:

$$\begin{gathered} \omega_0 \sim N\left(0.3,\ 0.1^2\right),\ \alpha_0 \sim N\left(0.1,\ 0.05^2\right),\ \beta_0 \sim N\left(0.05,\ 0.02^2\right),\ \gamma_0 \sim N\left(0.6,\ 0.05^2\right) \\ \theta_0 \sim N\left(\mu_\theta, \tau_\theta^2\right) \\ \sigma_\theta \sim C^+(0, b) \\ \sigma_{RV} \sim C^+(0, c) \\ \overset{\sim}{\theta}_t \sim N(0,1),\ t = 1, \ldots, N \end{gathered} \tag{10}$$

where $C^+(0, b)$ is the half-Cauchy distribution adjusted at 0 with scale b, and $(\mu_\theta,\ \tau_\theta)$ are prior mean and standard deviation hyperparameters.

Innovation standard deviations:

$$\sigma_\theta \sim Half - Cauchy(0, 0.1),\ \sigma_{RV} \sim Half - Cauchy(0, 0.2) \tag{11}$$

Random walk innovations:

$$\overset{\sim}{\theta}_t \sim N(0,1),\ t = 1, \ldots, N,\ \theta \in \{\omega, \alpha, \beta, \gamma\} \tag{12}$$

The Bayesian posterior of this model can be written as:

$$p(\theta_{1:N}, h_{1:N}, \sigma_{RV} | RV_{1:N}, JV_{1:N}) \propto \prod_{t=1}^{N} N\left(RV_t \middle| h_t, \sigma_{RV}^2\right).p(h_{1:N} | \theta_{1:N}, RV_{1:N}).p(\theta_{1:N}).p(\sigma_{RV}) \tag{13}$$

The mathematical properties of the BtvGARCH-Itô model are formally established in Appendix B, where we present the positivity and boundedness of h_t (Theorem A1), the properness of the Bayesian posterior (Theorem A2), the identifiability of time-varying parameters (Theorem A3), and posterior consistency under the true data-generating process (Theorem A4). These results ensure that this model is well-defined, interpretable, and capable of producing reliable inference in dynamic financial markets. Implementation details in R (version 4.5.1) are provided in the supplementary material.

4. Simulation Study

4.1. Data Generation Process

We simulated synthetic data for N = 100 and N = 200 time points to evaluate the model's finite sample performance. The jump variation process JV was generated as

independent draws from a uniform distribution on [0, 0.2] with the median value denoted by $\lambda_{\omega,\,L}$. The time-varying parameters $\omega_{g,t}$, $\alpha_{g,t}$, $\beta_{g,t}$, and γ_t were defined to vary smoothly over time, according to sinusoidal functions, to mimic realistic dynamics. The latent volatility h_t was computed recursively as follows:

$$\omega_{g,t} = 0.3 + 0.1sin\left(\frac{2\pi t}{N}\right),\ \alpha_{g,t} = 0.1 + 0.05\sin\left(\frac{4\pi t}{N}\right) \tag{14}$$

$$\beta_{g,t} = 0.05 + 0.03\sin\left(\frac{6\pi t}{N}\right), \gamma_t = 0.6 + 0.05cos\left(\frac{2\pi t}{N}\right) \tag{15}$$

With $JV_t \sim N(0, 0.2), \lambda_{\omega,L} = median(JV_t)$ and

$$h_1 = \frac{\omega_{g,1} + \beta_{g,1}.\lambda_{\omega_L}.}{max\left(10^{-6}, 1 - \alpha_{g,1} - \gamma_1\right)} \tag{16}$$

$$h_t = \omega_{g,t} + \gamma_t h_{t-1} + \alpha_{g,t} RV_{t-1} + \beta_{g,t} JV_{t-1},\ \ RV_t \sim N\left(h_t, 0.1^2\right) \tag{17}$$

4.2. Simulation Results

This section presents the performance of the BtvGARCH-Itô model compared to the original GARCH-Itô specification for two simulated data sample sizes. Table 1 presents the posterior mean estimates of the static parameters and their associated diagnostics, including posterior intervals, R hat values, and effective sample sizes. The posterior means for ω_g indicate the baseline level of volatility, α_g captures the impact of realized volatility, β_g measures the contribution of jumps, and γ reflects the persistence of latent volatility. Table 2 compares the estimated parameters from GARCH-Itô and BtvGARCH-Itô against the true parameter values. The results clearly show that the BtvGARCH-Itô posterior means are closer to the true values across all parameters and sample sizes, highlighting the model's improved estimation accuracy. Table 3 further confirmed this through prediction accuracy metrics (MAE, MSE, RMSE) in which the BtvGARCH-Itô model consistently achieves lower errors for both static coefficients and latent volatility h_t. Figures 1–10 present the posterior time-varying estimates of means and 95 percent credible intervals of parameters. In sum, these simulation results demonstrated that the BtvGARCH-Itô is capable of more accurately estimating volatilities under a realistic synthetic dataset. Furthermore, this model can be used to estimate both static and time-varying coefficients. Thus, it supports the practical application to volatility analysis in empirical financial markets.

Table 1. Posterior means, standard deviations, credible intervals, $\hat{R}$ values, and effective sample sizes.

Data	Parameter	Mean	Std. Dev.	q5	q95	$\hat{R}$	Bulk-ESS	Tail-ESS
$N = 100$	$logp(\theta\|Y)$	−44.4	14.7	−69	−20.5	1.00	1608	2191
	ω_g	0.353	0.0667	0.243	0.462	1.00	2932	2605
	α_g	0.106	0.0419	0.0375	0.177	1.00	2752	2037
	β_g	0.0479	0.0197	0.0163	0.0805	1.00	3811	1606
	γ	0.622	0.0430	0.552	0.692	1.00	4132	2806
	$\sigma_{\omega_{g,t}}$	0.0517	0.0335	0.00449	0.111	1.01	872	1424
	$\sigma_{\alpha_{g,t}}$	0.100	0.154	0.00626	0.260	1.00	1538	1820
	$\sigma_{\beta_{g,t}}$	0.297	2.17	0.00662	0.754	1.00	3653	2416
	σ_{γ_t}	0.0535	0.0328	0.00575	0.112	1.02	572	1300
	σ_{RV}	0.0994	0.00823	0.0866	0.114	1.00	4589	2661

Table 1. *Cont.*

Data	Parameter	Mean	Std. Dev.	q5	q95	$\hat{R}$	Bulk-ESS	Tail-ESS
$N = 200$	$logp(\theta\|Y)$	−63.3	20.7	−95.5	−28.2	1.00	1737	2308
	ω_g	0.348	0.0651	0.238	0.452	1.00	1735	2117
	α_g	0.0854	0.0394	0.0220	0.153	1.00	1478	1472
	β_g	0.0492	0.0199	0.0164	0.0825	1.00	3298	1393
	γ	0.628	0.0448	0.556	0.703	1.00	2697	2556
	$\sigma_{\omega_{g,t}}$	0.0308	0.0189	0.00286	0.0639	1.00	533	1361
	$\sigma_{\alpha_{g,t}}$	0.0693	0.0652	0.00613	0.172	1.00	1904	2205
	$\sigma_{\beta_{g,t}}$	0.166	0.591	0.00612	0.511	1.00	3297	2468
	σ_{γ_t}	0.0369	0.0195	0.00496	0.0688	1.01	374	668
	σ_{RV}	0.0992	0.00549	0.0906	0.108	1.00	3642	3119

Notes: Table 1 provides the posterior estimates of static parameters (ω_g, α_g, β_g, γ) from the BtvGARCH-Itô model for simulated datasets ($N = 100$ and $N = 200$). Posterior sampling was performed using four parallel Markov chains with 1000 iterations and each chain with 500 warm-ups. Computations were carried out using the *cmdstanr* interface to the *Stan* R package (The model code was implemented in R 4.5.1 and the supporting material is available online at https://www.preprints.org/manuscript/202507.1745/v1, accessed on 17 July 2015). The models converge well, as indicated by the convergence diagnostic test, in which the $\hat{R}$ values are less than 1.02 and the effective sample sizes are sufficient. $logp(\theta|Y)$ indicates the log posterior density evaluated at the posterior mean of the parameter vector θ, and $\sigma_{k_{g,t}}$ presents standards deviations of weakly informative priors for the posterior time-varying means estimated in this model. The time-varying posterior means estimates of BtvGARCH-Itô and their corresponding true parameter values are presented in Figures 1–10.

Table 2. Simulation study results: GARCH-Itô vs. Bayesian Time-varying GARCH-Itô models.

Parameter	True	$N = 100$		$N = 200$	
		GARCH-Itô	BtvGARCH-Itô	GARCH-Itô	BtvGARCH-Itô
ω	0.3	0.18661	0.353	0.16149	0.348
α	0.1	0.16321	0.106	0.05573	0.0854
β	0.05	0.0000004	0.0479	0.00000002	0.0492
γ	0.6	0.59281	0.622	0.74135	0.628

Notes: Table 2 shows both estimated and true parameter values to compare the performance of GARCH-Itô and BtvGARCH-Itô for simulated sample sizes $N = 100$ & $N = 200$. In both cases, BtvGARCH-Itô model estimates are closer to true parameter values.

Table 3. Model accuracy metrics: GARCH-Itô vs. Bayesian Time-varying GARCH-Itô.

Parameter	$N = 100$						$N = 200$					
	GARCH-Itô			BtvGARCH-Itô			GARCH-Itô			BtvGARCH-Itô		
	MAE	MSE	RMSE	MAE	MSE	RMSE	MAE	MSE	RMSE	MAE	MSE	RMSE
ω	0.1133	0.0128	0.1133	0.0432	0.00242	0.0492	0.1385	0.0191	0.1385	0.0469	0.0028	0.0529
α	0.0632	0.0039	0.0632	0.0289	0.0011	0.0339	0.0442	0.0019	0.0442	0.0346	0.0019	0.0440
β	0.0499	0.0024	0.0499	0.0198	0.0004	0.0218	0.0499	0.0024	0.0499	0.0188	0.0004	0.0212
γ	0.0072	0.0000	0.0071	0.0440	0.0033	0.0575	0.1413	0.0199	0.1413	0.0419	0.0023	0.0489
h_t	0.0568	0.0085	0.0922	0.0299	0.0012	0.0348	0.0535	0.0072	0.0848	0.0192	0.006	0.0253

Notes: Table 3 provides the forecast accuracy of both original GARCH-Itô and BtvGARCH-Itô models based on three error metrics: Mean Absolute Error (MAE), Mean Squared Error (MSE), and Root Mean Squared Error (RMSE). Accuracy is assessed for each key parameter and for the latent volatility using simulated samples $N = 100$ and $N = 200$. These results revealed that the BtvGARCH-Itô model achieves lower errors compared to the original GARCH-Itô.

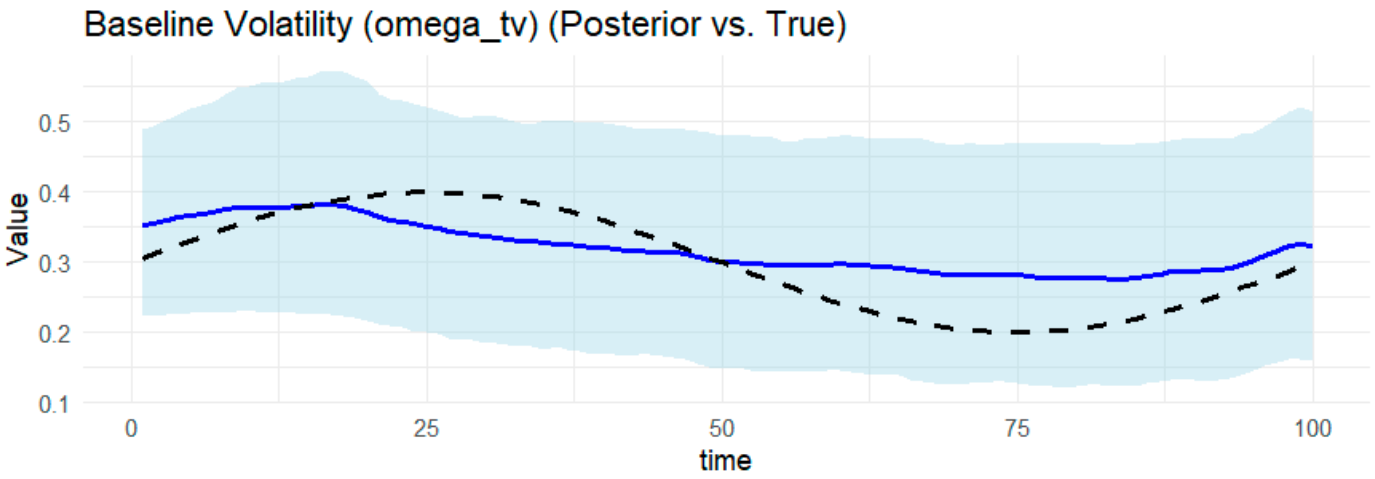

Figure 1. The time-varying posterior means of omega ($\omega_{g,t}$) estimated by the BtvGARCH-Itô model. Notes: The solid lines present true parameter values that are being used to generate the data (t = 100), and the dashed lines represent the time-varying posterior mean estimates.

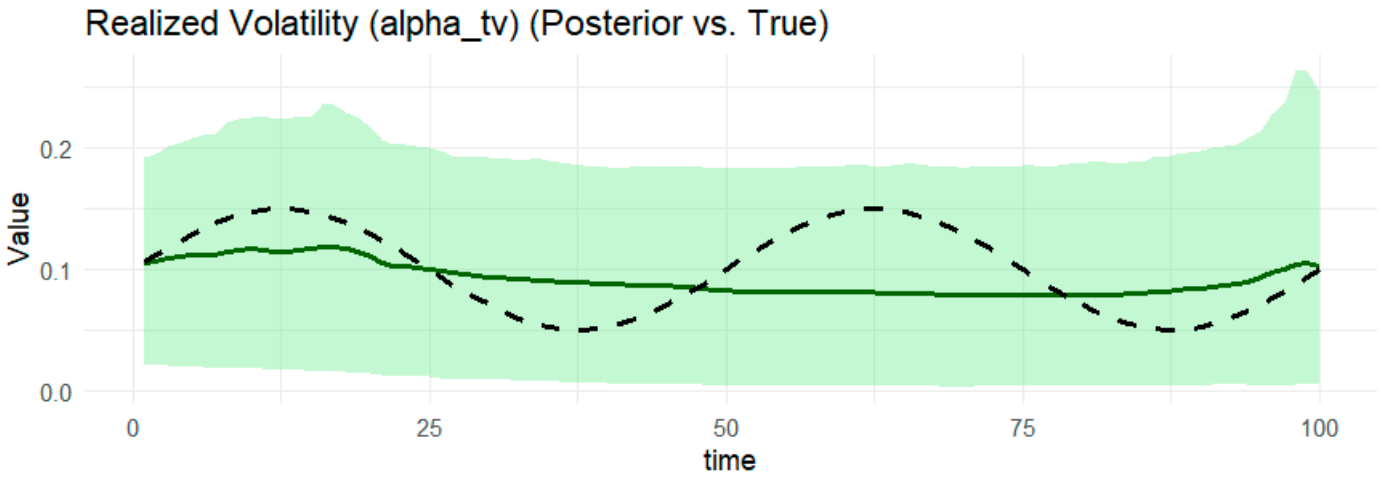

Figure 2. The time-varying posterior means of alpha ($\alpha_{g,t}$) estimated by the BtvGARCH-Itô model. Notes: The solid lines present true parameter values that are being used to generate the data (t = 100), and the dashed lines represent the time-varying posterior mean estimates.

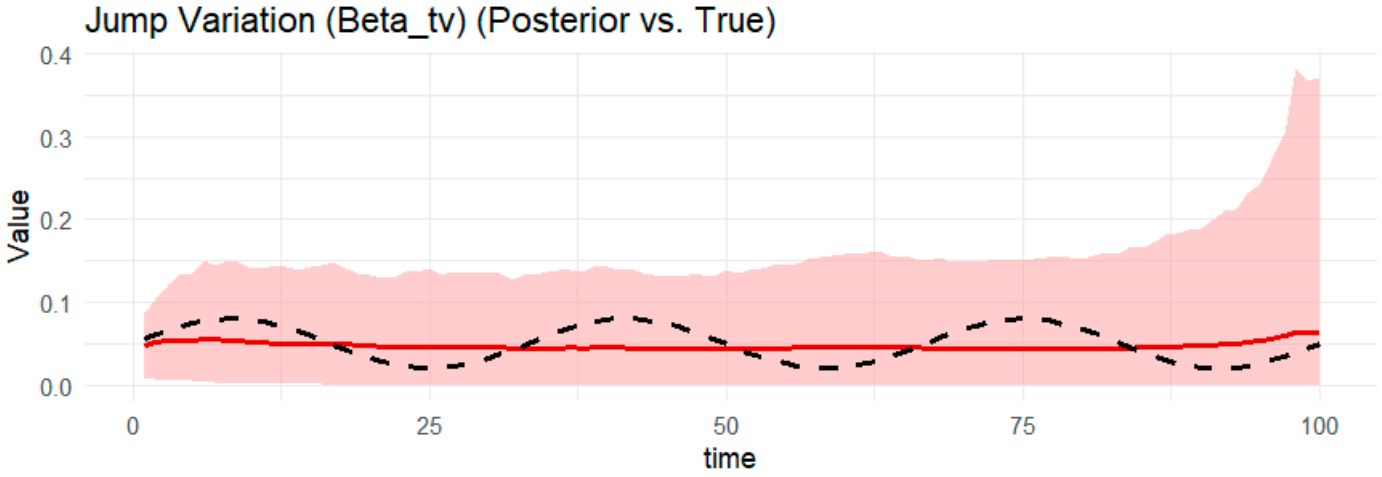

Figure 3. The time-varying posterior means of Beta ($\beta_{g,t}$) estimated by the BtvGARCH-Itô model. Notes: The solid lines present true parameter values that are being used to generate the data (t = 100), and the dashed lines represent the time-varying posterior mean estimates.

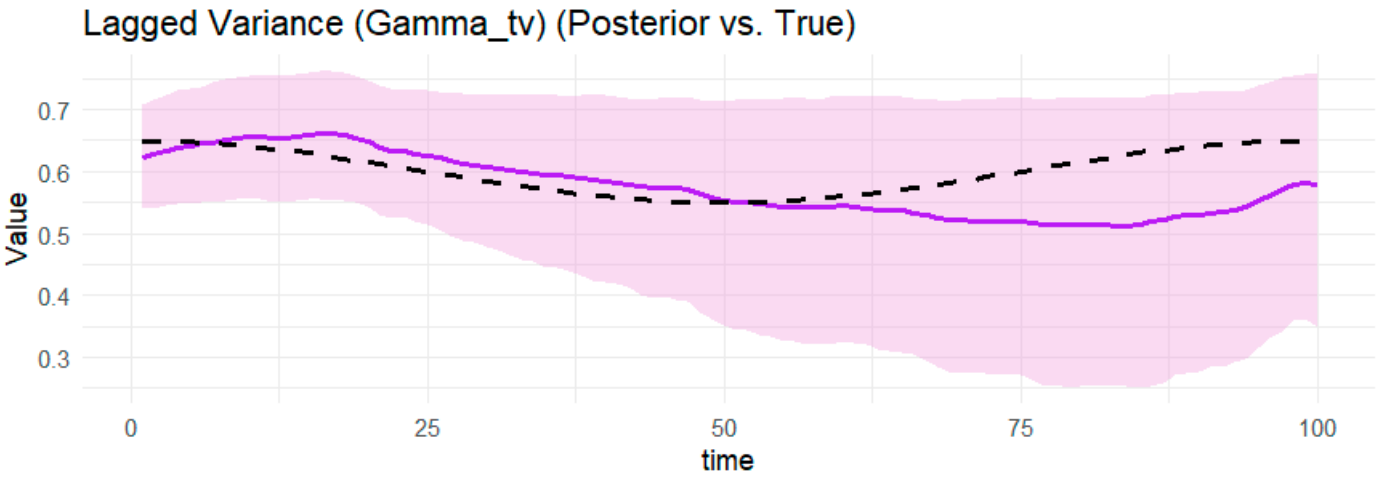

Figure 4. The time-varying posterior means of Gamma (γ_t) estimated by the BtvGARCH-Itô model. Notes: The solid lines present true parameter values that are being used to generate the data (t = 100), and the dashed lines represent the time-varying posterior mean estimates.

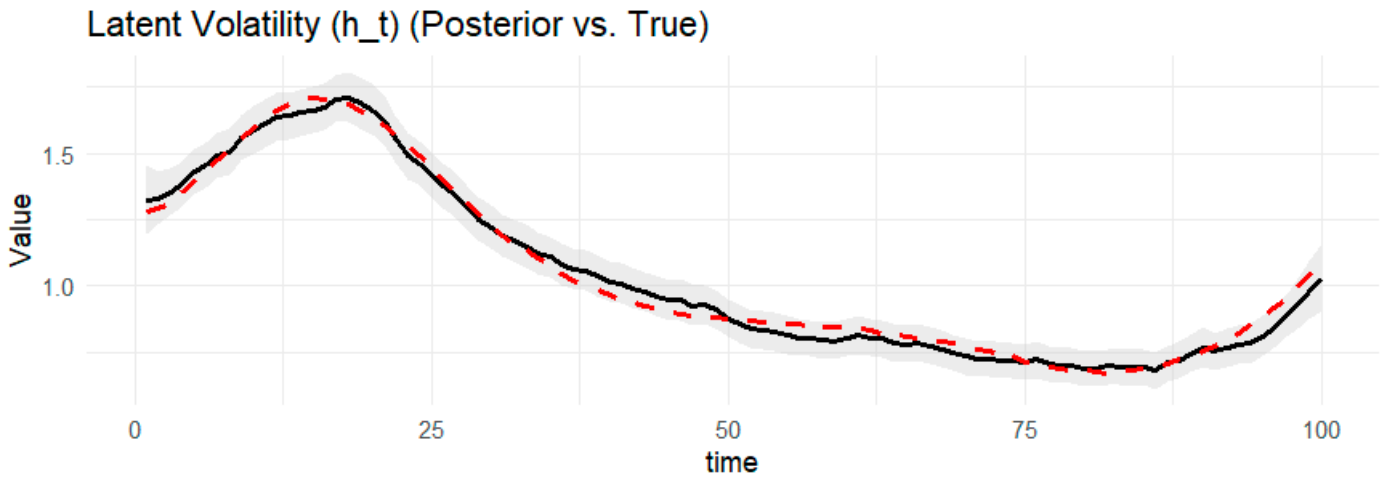

Figure 5. The time-varying posterior means of latent variance or factor (h_t) estimated by the BtvGARCH-Itô model. Notes: The solid lines present true parameter values that are being used to generate the data (t = 100), and the dashed lines represent the time-varying posterior mean estimates.

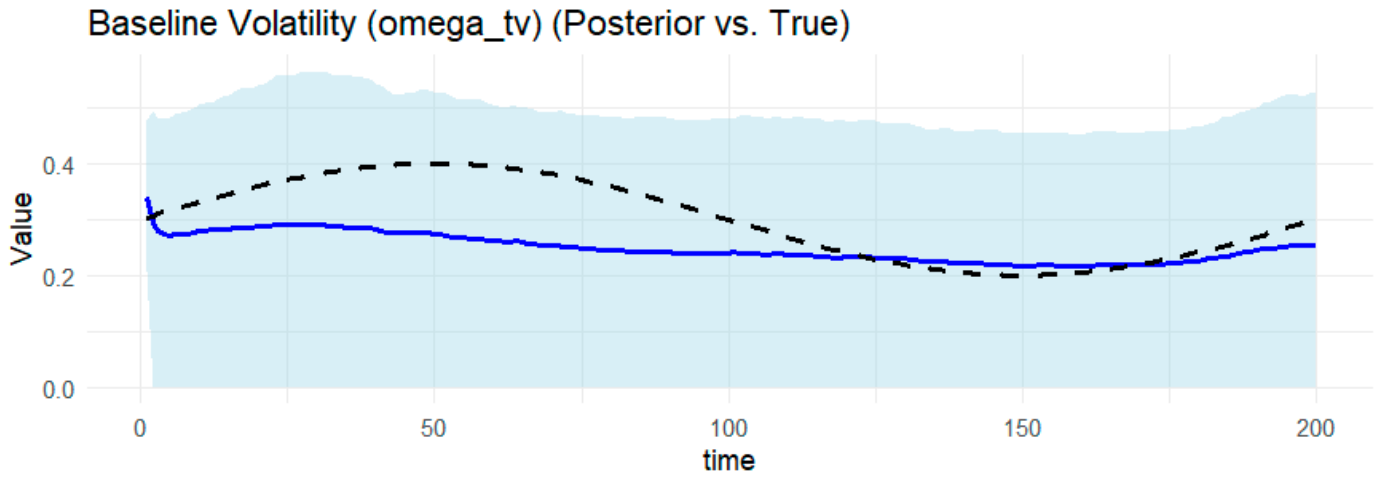

Figure 6. The time-varying posterior means of omega ($\omega_{g,t}$) estimated by the BtvGARCH-Itô model. Notes: The solid lines present true parameter values that are being used to generate the data (t = 200), and the dashed lines represent the time-varying posterior mean estimates.

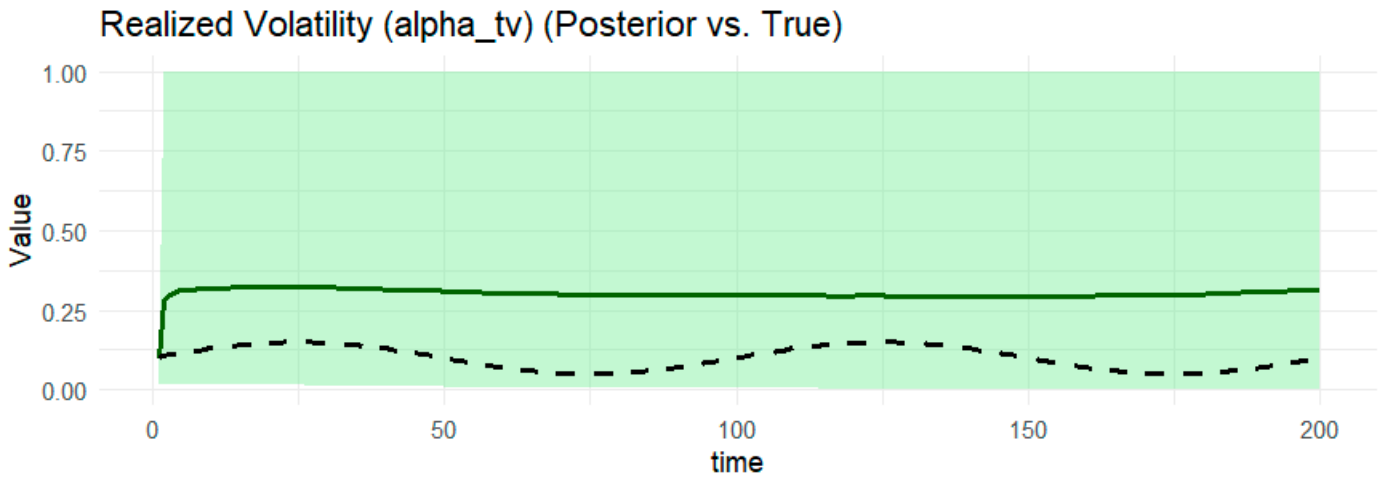

Figure 7. The time-varying posterior means of alpha ($\alpha_{g,t}$) estimated by the BtvGARCH-Itô model. Notes: The solid lines present true parameter values that are being used to generate the data (t = 200), and the dashed lines represent the time-varying posterior mean estimates.

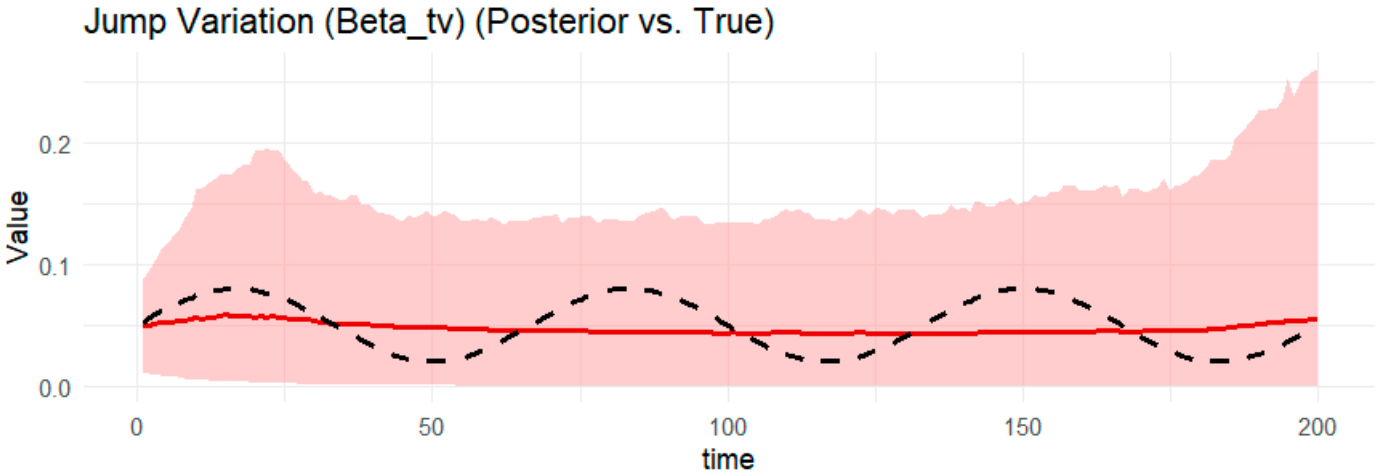

Figure 8. The time-varying posterior means of Beta ($\beta_{g,t}$) estimated by the BtvGARCH-Itô model. Notes: The solid lines present true parameter values that are being used to generate the data (t = 200), and the dashed lines represent the time-varying posterior mean estimates.

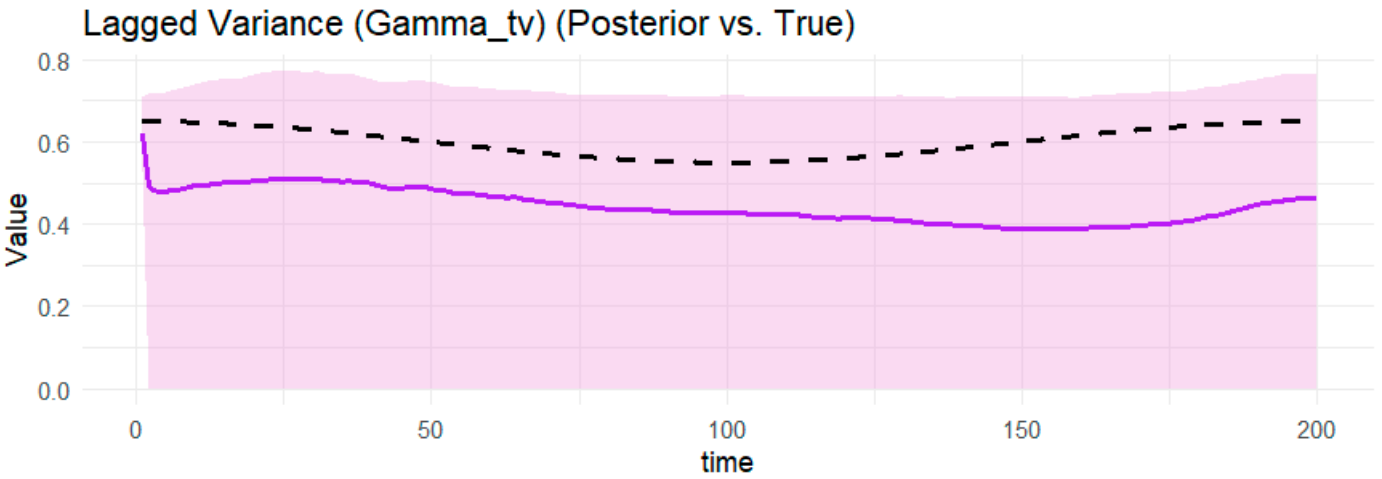

Figure 9. The time-varying posterior means of Gamma (γ_t) estimated by the BtvGARCH-Itô model. Notes: The solid lines present true parameter values that are being used to generate the data (t = 200), and the dashed lines represent the time-varying posterior mean estimates.

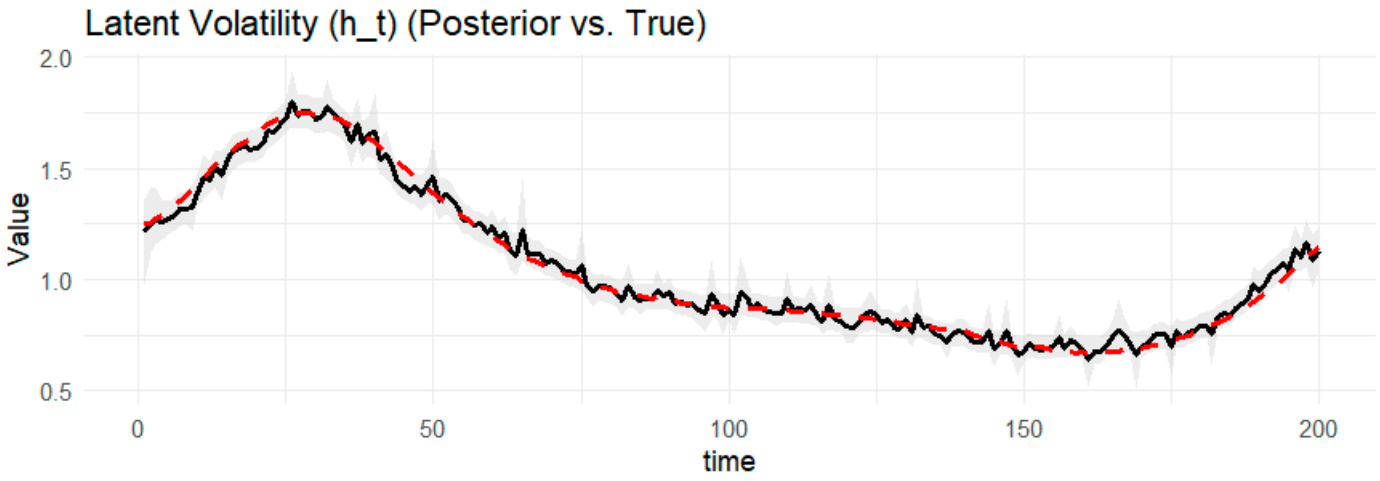

Figure 10. The time-varying posterior means of latent variance or factor (h_t) estimated by the BtvGARCH-Itô model. Notes: The solid lines present true parameter values that are being used to generate the data (t = 200), and the dashed lines represent the time-varying posterior mean estimates.

5. Empirical Study

This section presents the empirical application of the Bayesian Time-varying GARCH-Itô (BtvGARCH-Itô) model to two financial assets: the S&P 500 index and Bitcoin (BTC). The data consist of one-minute intraday returns. The S&P 500 sample spans 3 January 2023 to 31 December 2024 while the Bitcoin sample covers 1 January 2023, to 1 January 2025. The S&P 500 is a liquid and diversified equity benchmark in a regulated market. The chosen period reflects post-pandemic monetary tightening, inflation volatility, and the technology-driven equity rally in 2023–2024. Bitcoin is a decentralized and speculative digital asset, characterized by heavy tails and frequent jumps. The longer Bitcoin sample allows the capture of crypto-specific events, including the April 2024 halving and U.S. spot ETF approvals. The periods overlap but are not identical, reflecting different research aims: macroeconomic stabilization for equities and the full speculative cycle for Bitcoin. These choices provide economic and financial context. S&P 500 volatility responds to monetary policy announcements, inflation releases, and global shocks, while Bitcoin volatility reacts to regulatory news, market crashes, and speculative surges. The time-varying Bayesian framework detects these regime shifts and quantifies uncertainty around parameter changes.

For the case of S&P 500 (Table 4), it shows a strong empirical support for the model's effectiveness in studying the main features of volatility dynamics in a stable financial market. The static posterior intercept (ω_g), which sets the baseline level of conditional volatility, is estimated at 4.17×10^{-5}. The estimated average volatility level is low, which is consistent with the relatively stable U.S. equity market during the study period. The static posterior coefficient of realized volatility (α_g) is 0.0479. This value indicates a moderate impact of realized measures on volatility dynamics in the well-regulated market. The static posterior means of jump variation (β_g) is 0.0324, which assesses the influence of discontinuous price jumps on current volatility. The small positive value revealed that price jumps in the S&P 500 have a small effect on the overall volatility. The static posterior means estimated for lagged variance (γ) is 0.598, which measures the persistence of latent volatility.

Table 4. Posterior means, standard deviations, posterior intervals, $\hat{R}$ values, and effective sample sizes.

Parameter	Mean	Std. Dev.	q5	q95	$\hat{R}$	Bulk-ESS	Tail-ESS
$logp(\theta\|Y)$	3288	33	3235	3343	1.00	1216	427
ω_g	0.0000417	0.0000156	0.0000214	0.0000714	1.00	1193	426
α_g	0.0479	0.0336	0.00473	0.111	1.00	2878	4204
β_g	0.0324	0.0227	0.00118	0.0713	1.00	1867	2415
γ	0.598	0.0515	0.512	0.681	1.00	3211	4578
$\sigma_{\omega_{g,t}}$	0.0607	0.0457	0.00621	0.138	1.01	625	304
$\sigma_{\alpha_{g,t}}$	0.0399	0.0298	0.00315	0.0977	1.00	5547	3836
$\sigma_{\beta_{g,t}}$	0.0792	0.0356	0.0157	0.137	1.00	2179	1686
σ_{γ_t}	0.0467	0.0368	0.00397	0.118	1.00	2080	4168
σ_{RV}	0.000104	0.00000406	0.0000982	0.000110	1.00	782	282

Notes: Table 4 provides the posterior estimates of static parameters (ω_g, α_g, β_g, γ) from the BtvGARCH-Itô model for S&P 500 intraday returns between 3 January 2023 and 31 December 2024. Posterior sampling was performed using four parallel Markov chains with 2000 iterations and each chain with 1000 warm-ups. Computations were carried out using the *cmdstanr* interface to the *Stan* R package. The models converge well, as indicated by the convergence diagnostic test, in which the $\hat{R}$ values are less than 1.01, and the effective sample sizes are satisfactory. $logp(\theta|Y)$ indicates the log posterior density evaluated at the posterior mean of the parameter vector θ, and $\sigma_{k_{g,t}}$ presents standard deviations of weakly informative priors for the posterior time-varying means estimated in this model. The time-varying posterior means and 95 percent posterior intervals are presented in Figures 11–15.

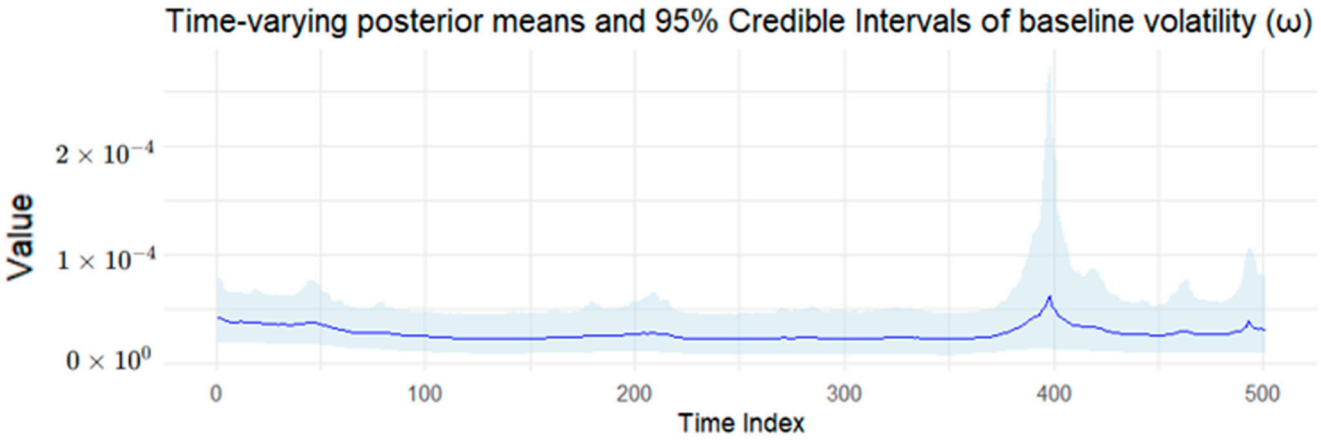

Figure 11. Time-varying posterior means of baseline volatility (S&P 500). Notes: It presents the time-varying posterior means (solid lines) and 95% credible intervals (shaded areas) for all parameters estimated from the BtvGARCH-Itô model using 1-min close prices of the S&P 500 from 3 January 2023 to 31 December 2024.

For the case of Bitcoin (Table 5), the static intercept posterior means for parameter (ω_g) is 2.11×10^{-4}. The estimated average volatility level is much larger than the S&P 500 index during the study period. This indicates how Bitcoin remains a speculative and risk-sensitive asset. The static posterior coefficient of realized volatility (α_g) is 0.0642, which also exceeds that of the S&P 500. This finding highlights Bitcoin's high volatility reactivity to incoming market information. The static posterior means of jump variation (β_g) is 0.00245, which is substantially lower than S&P 500 estimates. This result suggests that persistent price jumps contribute least to latent volatility. One possible reason is that the baseline and RV already absorb most of the high-frequency variation. The static posterior means estimate for lagged variance (γ) is 0.573, which is slightly less than in the equity market S&P 500. However, the larger baseline volatility in BTC highlights the adaptability of the model to differentiate the nature of high-risk and stable financial markets.

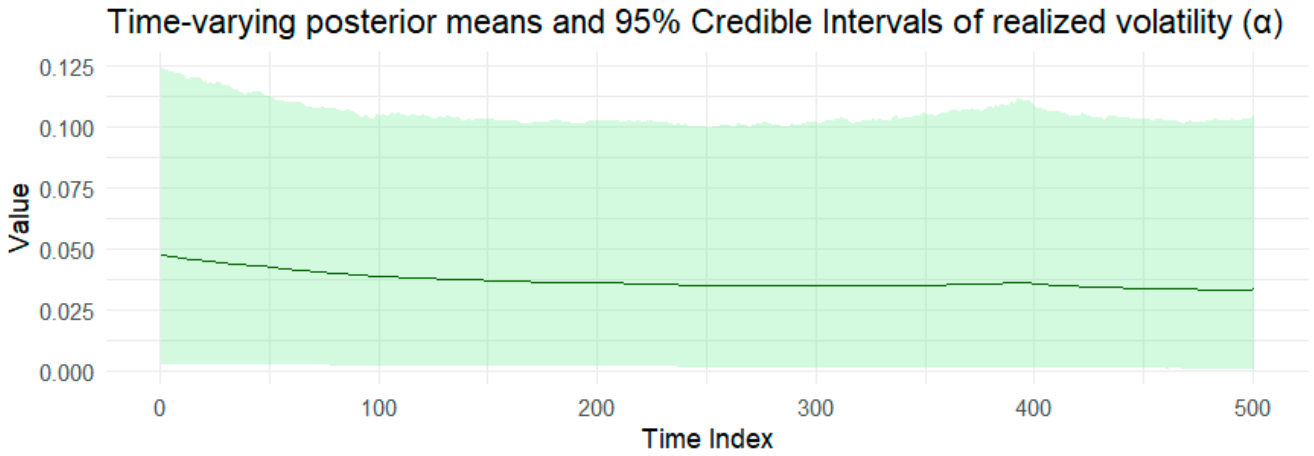

Figure 12. Time-varying posterior means of realized volatility (S&P 500). Notes: It presents the time-varying posterior means (solid lines) and 95% credible intervals (shaded areas) for all parameters estimated from the BtvGARCH-Itô model using 1-min close prices of the S&P 500 from 3 January 2023 to 31 December 2024.

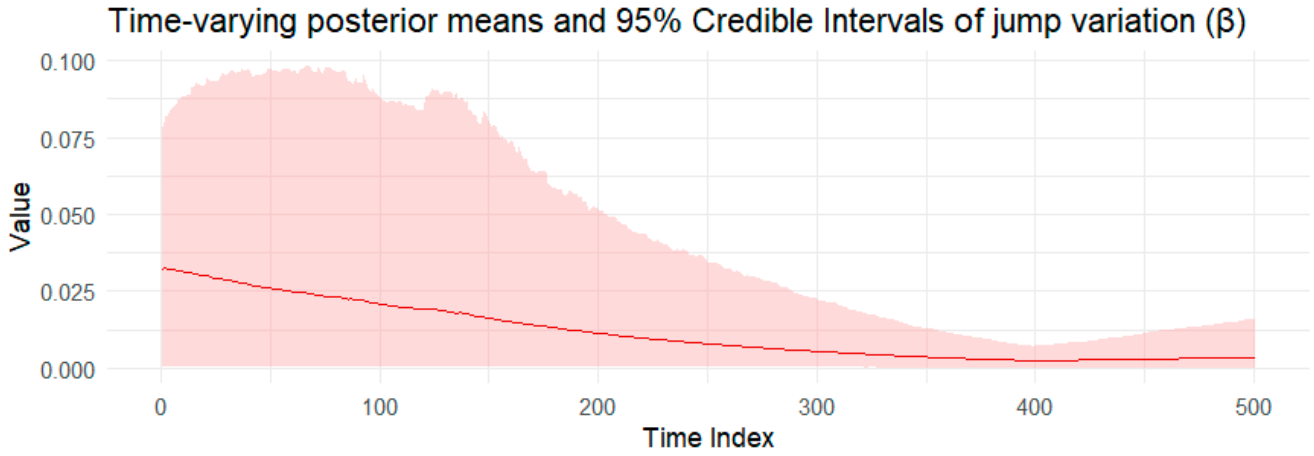

Figure 13. Time-varying posterior means of jump variation (S&P 500). Notes: It presents the time-varying posterior means (solid lines) and 95% credible intervals (shaded areas) for all parameters estimated from the BtvGARCH-Itô model using 1-min close prices of the S&P 500 from 3 January 2023 to 31 December 2024.

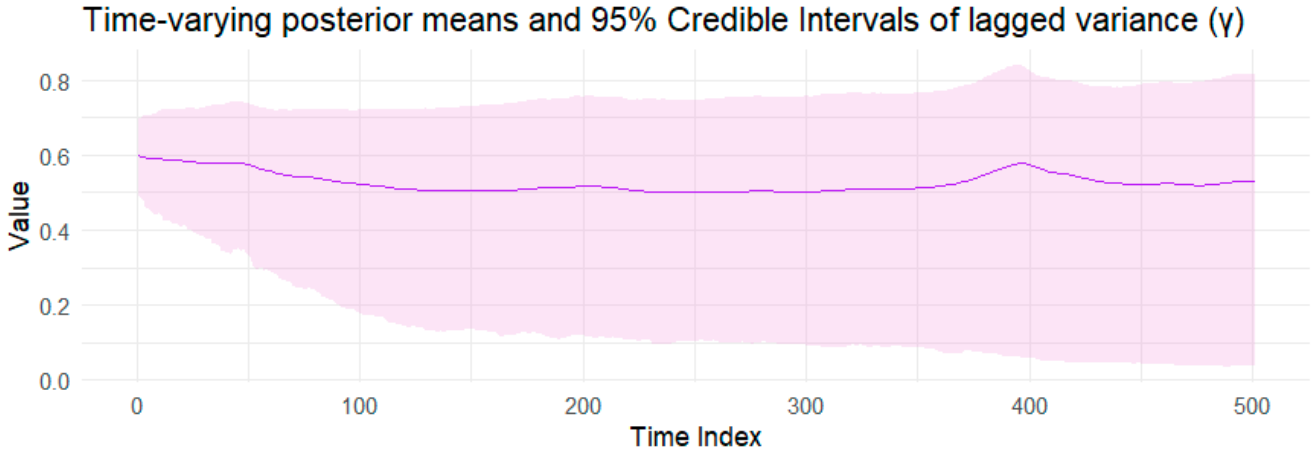

Figure 14. Time-varying posterior means of lagged variance (S&P 500). Notes: It presents the time-varying posterior means (solid lines) and 95% credible intervals (shaded areas) for all parameters estimated from the BtvGARCH-Itô model using 1-min close prices of the S&P 500 from 3 January 2023 to 31 December 2024.

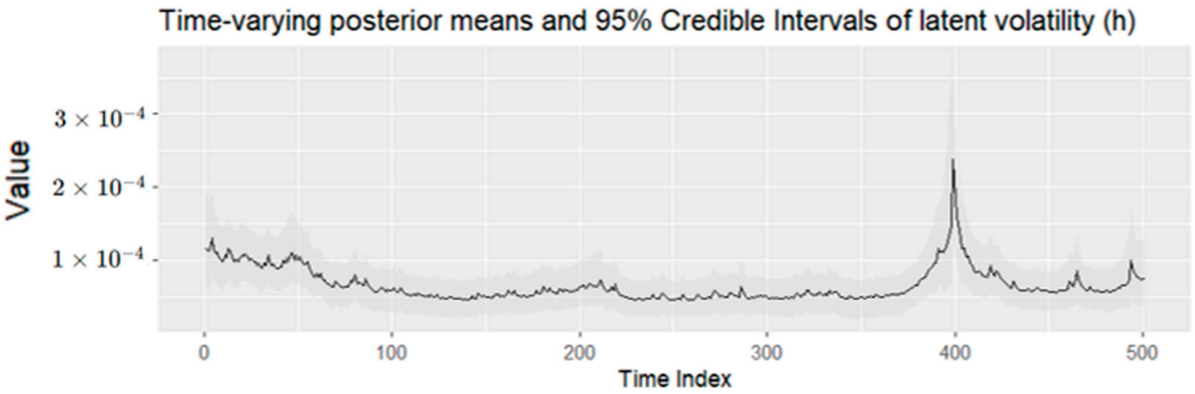

Figure 15. Time-varying posterior means of latent variance or factor (S&P 500). Notes: It presents the time-varying posterior means (solid lines) and 95% credible intervals (shaded areas) for all parameters estimated from the BtvGARCH-Itô model using 1-min close prices of the S&P 500 from 3 January 2023 to 31 December 2024.

Table 5. Posterior means, standard deviations, posterior intervals, $\hat{R}$ values, and effective sample sizes.

Parameter	Mean	Std. Dev.	q5	q95	$\hat{R}$	Bulk-ESS	Tail-ESS
$logp(\theta\|Y)$	3215	37.3	3153	3276	1.00	3114	4280
ω_g	0.000211	0.0000660	0.000116	0.000329	1.00	8057	5696
α_g	0.0642	0.0364	0.0112	0.131	1.00	5148	3616
β_g	0.00245	0.00397	0.0000656	0.00917	1.00	4538	4545
γ	0.573	0.0477	0.495	0.652	1.00	13,966	6050
$\sigma_{\omega_{g,t}}$	0.0265	0.0167	0.00308	0.0564	1.00	2445	3339
$\sigma_{\alpha_{g,t}}$	0.0417	0.0300	0.00341	0.0993	1.00	5523	4083
$\sigma_{\beta_{g,t}}$	0.04747	0.0344	0.00377	0.114	1.00	5144	3689
σ_{γ_t}	0.0397	0.0296	0.00351	0.0975	1.00	3763	4089
σ_{RV}	0.000944	0.0000252	0.000903	0.000987	1.00	18,236	5187

Notes: Table 5 provides the posterior estimates of static parameters (ω_g, α_g, β_g, γ) from the BtvGARCH-Itô model for Bitcoin (BTC) intraday returns between 1 January 2023 and 1 January 2025. Posterior sampling was performed using four parallel Markov chains with 2000 iterations and each chain with 1000 warm-ups. Computations were carried out using the *cmdstanr* interface to the *Stan* R package. The models converge well, as indicated by the convergence diagnostic test, in which $\hat{R}$ values are not greater than 1.00, and the effective sample sizes are satisfactory. $logp(\theta|Y)$ indicates the log posterior density evaluated at the posterior mean of the parameter vector θ, and $\sigma_{k_{g,t}}$ presents standard deviations of weakly informative priors for the posterior time-varying means estimated in this model. The time-varying posterior means and 95 percent posterior intervals are presented in Figures 16–20.

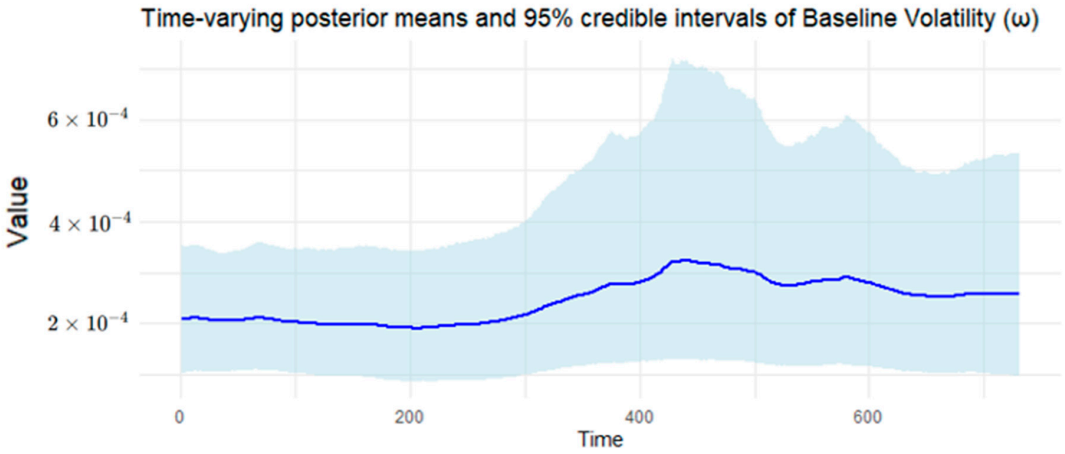

Figure 16. Time-varying posterior means of Baseline Volatility (Bitcoin). Notes: It presents the time-varying posterior means (solid lines) and 95% credible intervals (shaded areas) for all parameters estimated from the BtvGARCH-Itô model using 1-min close prices of Bitcoin (BTC) from 1 January 2023 to 1 January 2025.

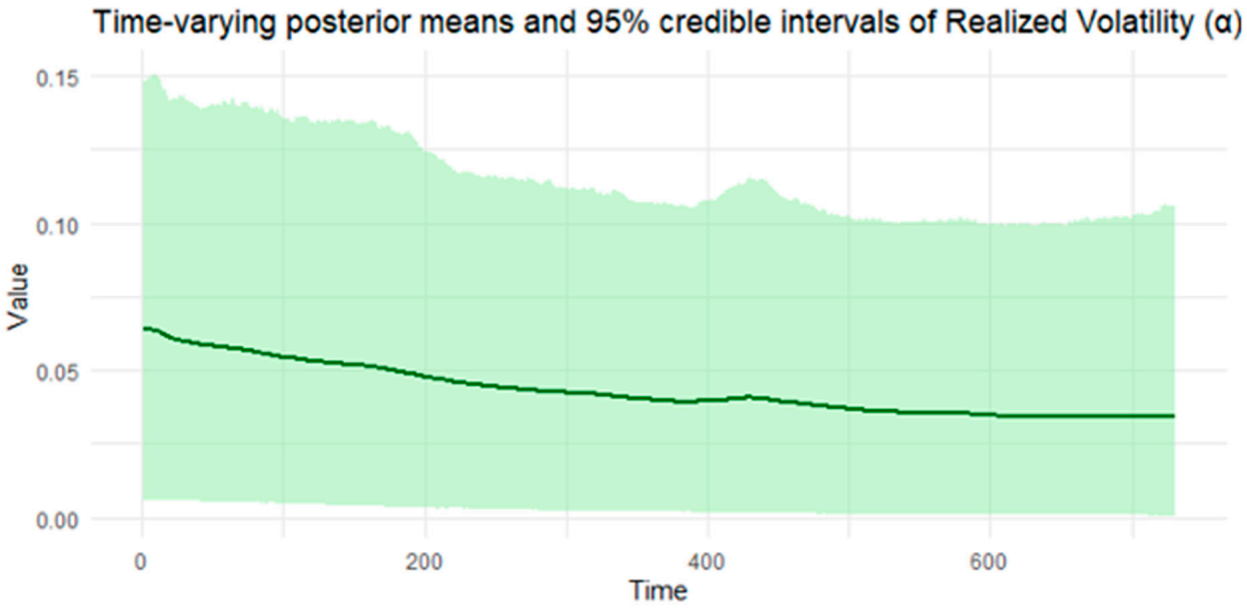

Figure 17. Time-varying posterior means of Realized Volatility (Bitcoin). Notes: It presents the time-varying posterior means (solid lines) and 95% credible intervals (shaded areas) for all parameters estimated from the BtvGARCH-Itô model using 1-min close prices of Bitcoin (BTC) from 1 January 2023 to 1 January 2025.

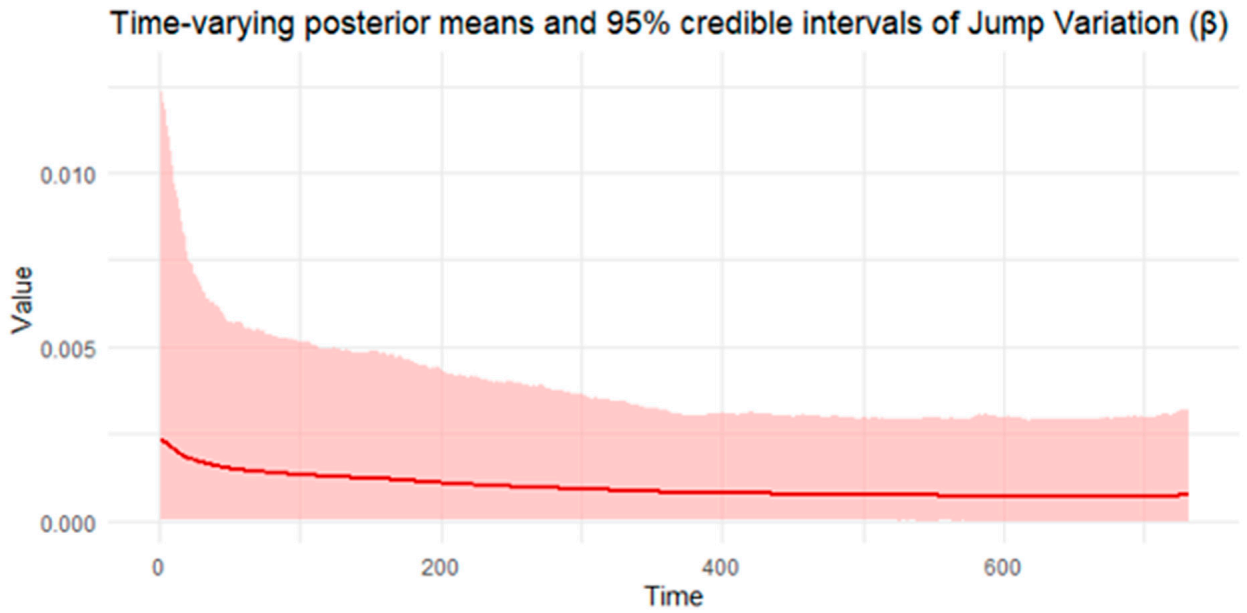

Figure 18. Time-varying posterior means of Jump Variation (Bitcoin). Notes: It presents the time-varying posterior means (solid lines) and 95% credible intervals (shaded areas) for all parameters estimated from the BtvGARCH-Itô model using 1-min close prices of Bitcoin (BTC) from 1 January 2023 to 1 January 2025.

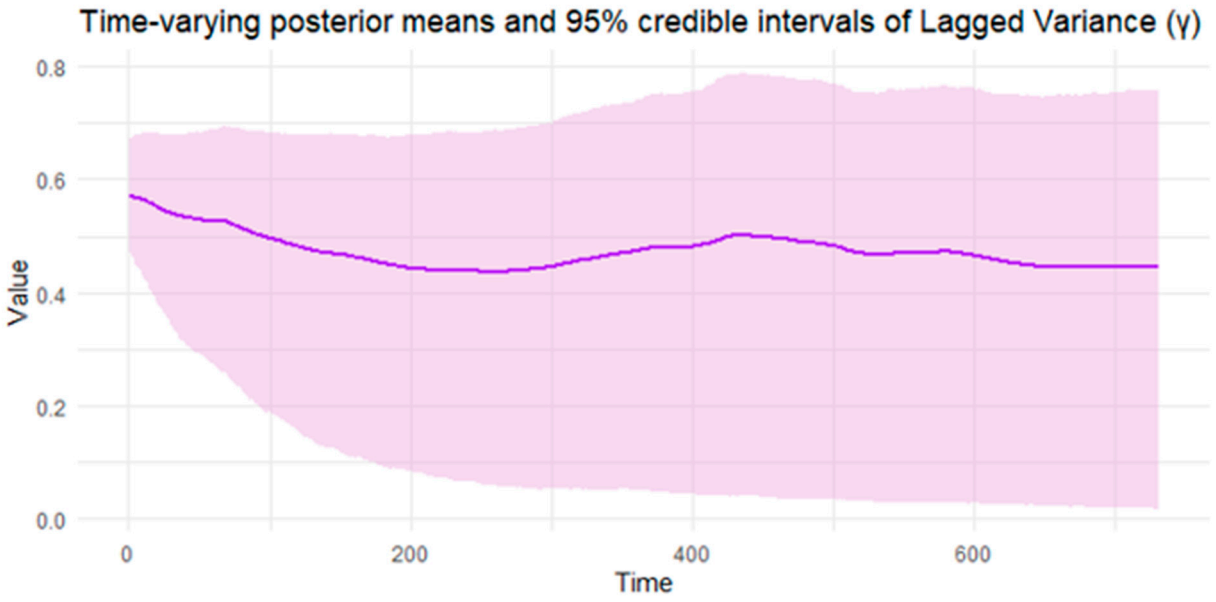

Figure 19. Time-varying posterior means of Lagged Variance (Bitcoin). Notes: It presents the time-varying posterior means (solid lines) and 95% credible intervals (shaded areas) for all parameters estimated from the BtvGARCH-Itô model using 1-min close prices of Bitcoin (BTC) from 1 January 2023 to 1 January 2025.

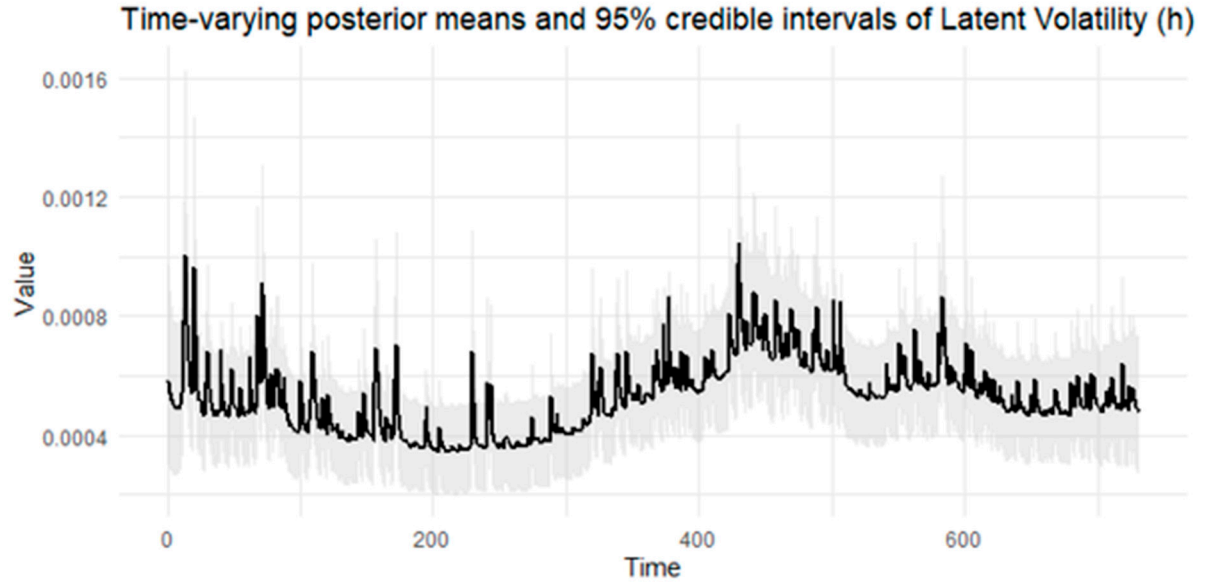

Figure 20. Time-varying posterior means of Latent Volatility or Factor (Bitcoin). Notes: It presents the time-varying posterior means (solid lines) and 95% credible intervals (shaded areas) for all parameters estimated from the BtvGARCH-Itô model using 1-min close prices of Bitcoin (BTC) from 1 January 2023 to 1 January 2025.

While the estimated static posterior means of the parameters present fixed volatility of the market, it proves overly restrictive in high-frequency data and continuously changing financial environments. This model addresses this by allowing parameters to vary over time to more accurately examine the dynamic nature of investor behavior, risk perceptions, and volatility transmission mechanisms. The time-varying estimates of the parameters, including latent volatility, are provided in Figures 11–15 for the S&P 500 and Figures 16–20 for Bitcoin. Those figures reveal intraday shifts in volatility, showing how realized volatility and latent components fluctuate over time. The time-varying estimates provide insights into regime changes and help capture short-term market responses to macroeconomic

announcements or shocks. With this method for modeling volatility persistence and shifts, investors can benefit from value-at-risk estimation and derivative pricing. The evidence from both assets supports the conclusion that while static models reveal the overall market behavior, time-varying models report unexpected shifts in volatility drivers that affect market risk. In sum, the empirical evidence validates the efficacy of the BtvGARCH-Itô model in analyzing dynamic volatility structures across both traditional and digital financial assets.

The empirical findings support the theoretical rationale of the BtvGARCH-Itô model. Static posterior estimates reflect baseline market characteristics: low average volatility in S&P 500 versus higher baseline volatility in Bitcoin, moderate influence of realized volatility, persistence captured by γ, and the relative contribution of jumps. Time-varying posterior estimates capture dynamic shifts in volatility. It revealed how latent variance, realized volatility, and jump effects vary over intraday intervals. These results validate that the model effectively operationalizes the time-varying latent volatility structure specified in the theoretical framework, accommodates high-frequency market features, and differentiates between stable (S&P 500) and speculative (Bitcoin) market behaviors. The empirical evidence, thus, confirms that the BtvGARCH-Itô model provides interpretable and reliable inference, consistent with its econometric specification.

6. Conclusions

This paper newly developed and empirically validated a Bayesian Time-varying Realized GARCH-Itô model, a novel framework that integrates discrete-time GARCH dynamics with continuous-time Itô processes and time-varying coefficients within Bayesian inference. This model advances volatility modeling because it allows model parameters to vary over time. Unlike original GARCH-Itô models that assume static coefficients, this BtvGARCH-Itô model enables joint inference on both static and time-varying posterior distributions. Additionally, this model offers a more flexible and accurate classification of volatility shifts through the use of latent stochastic components estimated for financial markets. This new model adds a significant contribution to the field of financial econometrics and financial volatility analysis.

Simulation studies conducted for sample sizes $N = 100$ and $N = 200$ determine how well this model recovered both static and time-varying parameters. In particular, the Bayesian posterior estimates closely track the true latent volatility path. The estimated simulation results confirmed that the BtvGARCH-Itô model achieves greater in-sample fit and out-of-sample forecast accuracy. This is evident in its closer alignment with true parameter values and lower error metrics (MAE, MSE, RMSE) compared to the original GARCH-Itô specification (Song et al., 2020). This model is also capable of tracking volatility shifts and identifying distinct volatility spikes linked to market shocks in the empirical application of volatility analysis of S&P 500 intraday returns. Furthermore, its application with Bitcoin returns demonstrates that the BtvGARCH-Itô can be applied to markets with heavy tails and frequent jumps.

Overall, this model offers a statistical tool for risk management and portfolio allocation in modern financial markets. It unifies time-varying parameters of realized volatility and jump variation within a full Bayesian posterior framework. While the BtvGARCH-Itô demonstrates strong performance in modeling volatility dynamics of high-frequency financial market returns, this study has several limitations. It focuses on only two assets, assumes time-invariant parameters for some components, and uses fixed bandwidths. Forecasts and risk measures rely on posterior estimates, which may be sensitive to data quality, priors, or structural breaks. Practical implementation of the model for multivariate or high-frequency applications involves substantial computational cost. Moreover, gen-

eralization to other markets or asset classes should be undertaken cautiously, as market microstructures, regulatory regimes, or extreme events may affect model performance. Future research could extend the model to multivariate settings to explore volatility spillovers and co-jumps, incorporate heavy-tailed distributions to better capture extreme events, or include macro-financial covariates to enhance forecasting accuracy.

The BtvGARCH-Itô is just the first step, and several directions remain open. In financial markets, assets move together, so extending this model to a multivariate setting would benefit further volatility spillovers and co-jumps, which are essential for portfolio risk assessment and cross-asset dynamics for investors. In practical applications, a fixed bandwidth might limit flexibility. Thus, allowing data-driven bandwidths could improve the accuracy of time-varying coefficient estimates. As fat tails exist in financial returns, incorporating heavy-tailed or skewed distributions, for example, Student-t distribution, may better catch extreme events or price jumps.

Supplementary Materials: The following supporting information can be downloaded at: https://www.mdpi.com/article/10.3390/econometrics13030034/s1.

Author Contributions: Conceptualization, methodology, software, validation, formal analysis, investigation, resources, data curation, writing—original draft preparation, writing—review and editing, visualization, supervision, project administration, funding acquisition, P.P. and H.K. All authors have read and agreed to the published version of the manuscript.

Funding: This research received no external funding.

Data Availability Statement: The empirical analysis in this study utilizes secondary data obtained from Yahoo Finance. Specifically, we downloaded intraday price data at 1-min intervals and computed log returns based on closing prices.

Acknowledgments: The authors have thoroughly reviewed and edited all content generated during the preparation of this manuscript and take full responsibility for its accuracy and conclusions. This study used only publicly available data and did not require ethical approval. Grok AI was used only for grammar and language improvements.

Conflicts of Interest: The authors declare no conflicts of interest.

Appendix A

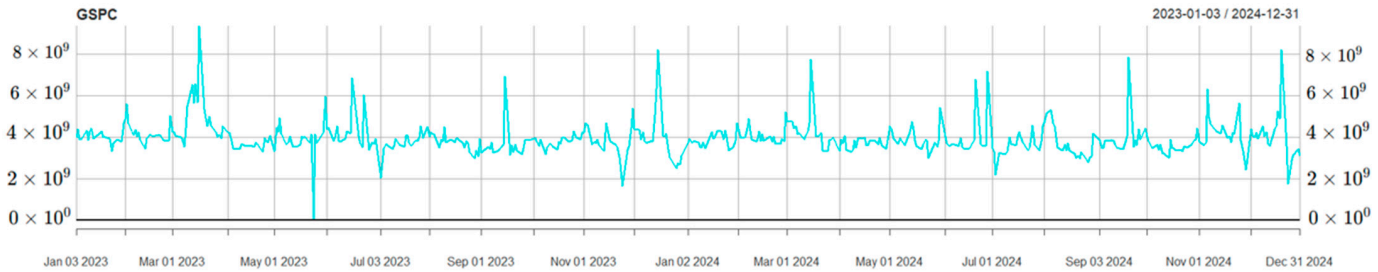

Figure A1. S&P 500 close prices (1-min frequency data) from 3 January 2023 to 31 December 2024.

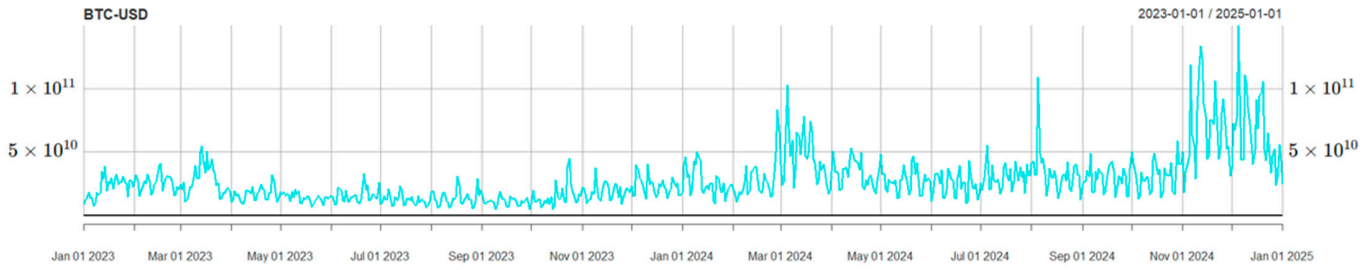

Figure A2. Bitcoin close prices (1-min frequency data) from 3 January 2023 to 1 January 2025.

Appendix B. Theorems and Proofs

Theorem A1. *Positivity and Boundedness of the Latent Volatility Process.*

Assume $\omega_t, \alpha_t, \beta_t, \gamma_t \in (0,1)$, $\omega_t + \gamma_t < 1$, RV_t, $JV_t \in [0, M]$ *for some* $M < \infty$, *and* $h_1 > 0$. *Then, the latent volatility process* $\{h_t\}_{t=1}^{N}$ *satisfies:*

$$0 < h_t \leq \frac{max_t(\omega_t + M(\alpha_t + \beta_t))}{1 - max_t.\gamma_t} \leq H < \infty$$

Proof of Theorem A1. We prove positivity and boundedness by induction.

Base case (t = 1): The initial volatility is:

$$h_1 = \frac{\omega_1 + \beta_1 \lambda_{\omega,\, L}}{max(e,\, 1 - \alpha_1 - \gamma_1)}$$

Since $\omega_1 + \beta_1 \lambda_{\omega,L} > 0$ and $\max(e, 1 - \alpha_1 - \gamma_1) > 0$, we have $h_1 > 0$. For boundedness:

$$h_1 \leq \frac{\omega_1 + \beta_1 \lambda_{\omega,\, L}}{1 - \alpha_1 - \gamma_1)} \leq \frac{1 + \lambda_{\omega,\, L}}{e} = \overline{h}_1$$

where $\overline{h}_1 < \infty$ since $e > 0$ and $\lambda_{\omega,\, L}$ is a finite constant.

Assume $h_{t-1} > 0$ and $h_{t-1} < \overline{h}_{t-1}$. For $t \geq 2$

$$h_1 = \omega_t + \alpha_t RV_{t-1} + \beta_t JV_{t-1} + \gamma_t h_{t-1}$$

Since $\omega_t, \alpha_t, \beta_t, \gamma_t \in (0,1)$, $RV_{t-1}, JV_{t-1} \geq 0$ and $h_{t-1} > 0$, it follows that $h_t \geq \omega_t > 0$. For boundedness:

$$h_t \leq \omega_t + \alpha_t M + \beta_t M + \gamma_t \overline{h}_{t-1} \leq 1 + M(\alpha_{t-1} + \beta_{t-1}) + \gamma_t \overline{h}_{t-1}$$

Iterate the inequality:

$$h_t \leq \omega_t + M(\alpha_t + \beta_t) + \gamma_t[\omega_{t-1} + M(\alpha_{t-1} + \beta_{t-1}) + \gamma_{t-1} h_{t-2}]$$

Continuing to t = 1, we obtain:

$$h_t \leq \sum_{k=0}^{t-2} \left(\prod_{j=1}^{k} \gamma_{t-j} \right) [\omega_{t-k} + M(\alpha_{t-k} + \beta_{t-k})] + \left(\prod_{j=1}^{t-1} \gamma_{t-j} \right) h_1$$

Since $\gamma_t < 1$, the series converges. Bounding each term:

$$\omega_t + M(\alpha_t + \beta_t) \leq 1 + 2M,\ h_1 \leq \overline{h}_1, \prod_{j=1}^{t-1} \gamma_{t-j} \leq \left({}^{max}_{t} \gamma_t \right)^k \overline{h}_t$$

Then, we obtain:

$$h_t \leq \sum_{k=0}^{t-2} \left({}_t^{max}\gamma_t\right)^k (1+2M) + \left({}_t^{max}\gamma_t\right)^{t-1} \overline{h}_t$$

The geometric series converges since ${}_t^{max}\gamma_t < 1$:

$$\sum_{k=0}^{\infty} \left({}_t^{max}\gamma_t\right)^k = \frac{1}{1 - {}_t^{max}\gamma_t}$$

Thus:

$$h_t \leq \frac{1+2M}{1-{}_t^{max}\gamma_t} + \frac{\overline{h}_1}{(1-{}_t^{max}\gamma_t)^{t-1}} \leq \frac{{}_t^{max}(\omega_t + M(\alpha_t+\beta_t))}{1-{}_t^{max}\gamma_t} + \overline{h}_1 \leq \overline{h}$$

where $\overline{h} < \infty$. Hence, h_t is positive and bounded. □

Theorem A2. *Properness of the Bayesian Posterior Distribution.*

Given priors $\omega_0 \sim N(0.3, 0.1^2)$, $\alpha_0 \sim N(0.1, 0.05^2)$, $\beta_0 \sim N(0.05, 0.02^2)$, $\gamma_0 \sim N(0.6, 0.05^2)$, $\sigma_\theta \sim Half-Cauchy(0, 0.1)$, *for* $\theta \in \{\omega, \alpha, \beta, \gamma\}$ *and* $\sigma_{RV} \sim Half-Cauchy(0,\ 0.2)$, *and the posterior:*

$$p(\theta_{1:N}, h_{1:N}, \sigma_{RV} | RV_{1:N}, JV_{1:N})$$

is proper, i.e., $\int p(\theta_{1:N}, h_{1:N}, \sigma_{RV} | RV_{1:N}, JV_{1:N}).d\theta_{1:N}, dh_{1:N}, d\sigma_{RV} < \infty$.

Proof of Theorem A2. The joint posterior is:

$$p(\theta_{1:N}, h_{1:N}, \sigma_{RV} | RV_{1:N}, JV_{1:N}) \propto \left(\prod_{t=1}^{N} \frac{1}{\sqrt{2\pi\sigma_{RV}^2}} exp\left(-\frac{(RV_t - h_t)^2}{2\pi\sigma_{RV}^2} \right) \right) .\delta(h_{1:N} | \theta_{1:N}, RV_{1:N}, JV_{1:N}).p(\theta_{1:N}).p(\sigma_{RV})$$

Likelihood: The Gaussian likelihood is continuous and bounded for $\sigma_{RV} > 0$, and $h_t \in \left(0, \overline{h}\right)$ is finite by Theorem A1. Thus, it is integrable over any compact interval $RV_t \in [0, M]$.

Volatility Process: The Dirac delta $\delta(h_{1:N}|.)$ imposes deterministic recursion.

$$h_t = \frac{\omega_1 + \beta_1 \lambda_{\omega,\, L}}{max(e,\ 1-\alpha_1-\gamma_1)}, h_1 = \omega_t + \alpha_t RV_{t-1} + \beta_t JV_{t-1} + \gamma_t h_{t-1}$$

Thus, integrating out $h_{1:N}$ contributes to 1. □

Priors: Initial parameters $\theta_0 \sim N(.,.)$ are proper, the logit transformation ensures $\theta_t \in (0,1)$ and time-varying function follows a Gaussian random walk ($\theta_t^{raw} = \theta_{t-1}^{raw} + \sigma_\theta \acute{\theta}_t$) which defines a proper transition density.

Theorem A3. *Identifiability of Time-Varying Parameters. The mapping* $\theta_{1:N} \to h_{1:N} \to RV_{1:N}$ *is injective almost surely. That is, if* $\theta_{1:N} \neq \acute{\theta}_{1:N}$, *then* $p(RV_{1:N}|\theta_{1:N}) \neq p(RV_{1:N}|\acute{\theta}_{1:N})$ *with probability 1.*

Proof of Theorem A3. Let $\theta_{1:N}(\omega_{1:N}, \alpha_{1:N}, \beta_{1:N}, \gamma_{1:N}) \neq \acute{\theta}_{1:N}(\omega_{1:N}, \alpha_{1:N}, \beta_{1:N}, \gamma_{1:N})$. Let t_0 be the smallest index where $\theta_{t_0} \neq \acute{\theta}_{t_0}$.

Case $t_0 = 1$;

$$h_1 \leq \frac{\omega_1 + \beta_1 \lambda_{\omega,\, L}}{max(e, 1 - \alpha_1 - \gamma_1)},\ \acute{h}_1 \leq \frac{\acute{\omega}_1 + \acute{\beta}_1 \acute{\lambda}_{\omega,\, L}}{max(e, 1 - \acute{\alpha}_1 - \acute{\gamma}_1)}$$

This function f($\omega_1, \alpha_1, \beta_1, \gamma_1$) is continuously differentiable with non-zero partial derivatives (since $\lambda_{\omega,\, L} > 0$ and the denominator is positive). Hence, $\theta_1 \neq \acute{\theta}_1$ implies $h_1 \neq \acute{h}_1$.

Case $t_0 \geq 2$: for t < t_0, assume $h_1 = \acute{h}_1$ at t = t_0.

$$h_{t_0} = \omega_{t_0} + \alpha_{t_0} RV_{t_0-1} + \beta_{t_0} JV_{t_0-1} + \gamma_{t_0} h_{t_0-1} \acute{h_{t_0}} = \acute{\omega_{t_0}} + \acute{\alpha_{t_0}} \acute{RV_{t_0-1}} + \acute{\beta_{t_0}} \acute{JV_{t_0-1}} + \acute{\gamma_{t_0}} \acute{h_{t_0-1}}$$

Since $h_{t_0} = \acute{h_{t_0}}$ and $\theta_{t_0} = \acute{\theta_{t_0}}$, the linear combination differs for almost all RV_{t_0-1}, JV_{t_0-1} that implies $h_{t_0} \neq \acute{h_{t_0}}$. Since $RV_t \sim N(h_t, \sigma^2_{RV}), h_{t_0} \neq \acute{h_{t_0}}$ implies N $(h_t, \sigma^2_{RV}) \neq$ N $(\acute{h}_t, \acute{\sigma}^2_{RV})$, so $p(RV_{1:N}|\theta_{1:N}) \neq p(RV_{1:N}|\acute{\theta}_{1:N})$ almost surely. □.

Theorem A4. *Posterior Consistency under True Data Generation Process. (Let* $\{RV_t, JV_t\}_{t=1}^N$ *be generated from the true BtvGARCH-Itô process:* $RV_t \sim \left(\check{h}_t, \check{\sigma}^2_{RV}\right), \check{\omega}_t + \check{\alpha}_t \check{RV}_t + \check{\beta}_t \check{JV}_t + \check{\gamma}_t \check{h}_{t-1}$ *with true latent parameters* $\check{\theta}_{1:N}$ $(\check{\omega}_t, \check{\alpha}_t, \check{\beta}_t, \check{\gamma}_t)_{t=1}^N$, $\check{\sigma}_{1:N} > 0$. *Suppose the prior* Π: *over* $\theta_{1:N}$, σ_{RV} *assign positive density in every open neighborhood of* $(\check{\theta}_{1:N}, \check{\sigma}_{RV})$, *the likelihood* $p(RV_{1:N}|\theta_{1:N}, \sigma_{RV})$ *is continuous in* $(\theta_{1:N}, \sigma_{RV})$, *the parameter space is compact and the model is identifiable as shown in Theorem A3. Then, the posterior distribution satisfies:*

$$p(\theta_{1:N}, \sigma_{1:N}|RV_{1:N}, JV_{1:N}) \underset{\rightarrow}{d} \delta_{\check{\theta}, \check{\sigma}_{RV}}$$

i.e., the posterior weakly converges to a Dirac delta at the true parameters.

Proof of Theorem A4. We apply the posterior consistency result from Theorem 2.1 of Ghosal et al. (2000), which provides sufficient conditions under which Bayesian posterior lies on the true parameter values. Let Θ denote the parameter space for $(\theta_{1:N}, \sigma_{RV})$, and let $\Pi(.)$ be the prior. Let the posterior be defined as:

$$p(\theta_{1:N}, \sigma_{1:N}|RV_{1:N}, JV_{1:N}) \propto p(RV_{1:N}|\theta_{1:N}, \sigma_{1:N}).\Pi(\check{\theta}_{1:N}, \check{\sigma}_{RV})$$

Under the following conditions:

(i) The true parameter values $(\check{\theta}_{1:N}, \check{\sigma}_{RV})$ lie in the support of the prior Π;
(ii) The likelihood is continuous in $(\theta_{1:N}, \sigma_{RV})$;
(iii) The parameter space is compact $\theta_t \in (0,1)^4$ via logit transform and $\sigma_{RV} > 0$;
(iv) The model is identifiable (Theorem A3).

Then, the posterior distribution satisfies weak consistency:

$$p(\theta_{1:N}, \sigma_{1:N}|RV_{1:N}, JV_{1:N}) \underset{\rightarrow}{d} \delta_{\check{\theta}, \check{\sigma}_{RV}},\ as\ N \to \infty$$

□

References

Andersen, T. G., & Bollerslev, T. (1997). Intraday periodicity and volatility persistence in financial markets. *Journal of Empirical Finance*, *4*, 115–158. [CrossRef]

Andersen, T. G., Bollerslev, T., & Diebold, F. X. (2007). Roughing it up: Including jump components in the measurement, modeling, and forecasting of return volatility. *The Review of Economics and Statistics*, *89*(4), 701–720. [CrossRef]

Andersen, T. G., Thyrsgaard, M., & Todorov, V. (2019). Time-varying periodicity in intraday volatility. *Journal of the American Statistical Association*, *114*(528), 1695–1707. [CrossRef]

Barndorff-Nielsen, O. E., Hansen, P. R., Lunde, A., & Shephard, N. (2008). Designing realized kernels to measure ex-post variation of equity prices in the presence of noise. *Econometrica*, *76*(6), 1481–1536. [CrossRef]

Barndorff-Nielsen, O. E., & Shephard, N. (2004). Power and bipower variation with stochastic volatility and jumps. *Journal of Financial Econometrics*, *2*(1), 1–37. [CrossRef]

Bollerslev, T. (1986). Generalized autoregressive conditional heteroskedasticity. *Journal of Econometrics*, *31*(3), 307–327. [CrossRef]

Carr, P., & Wu, L. (2003). What type of process underlies options? A simple robust test. *The Journal of Finance*, *58*(6), 2581–2610. [CrossRef]

Engle, R. F. (1982). Autoregressive conditional heteroscedasticity with estimates of the variance of United Kingdom inflation. *Econometrica*, *50*(4), 987–1007. Available online: https://www.jstor.org/stable/1912773 (accessed on 20 May 2025). [CrossRef]

Engle, R. F., & Gallo, G. M. (2006). A multiple indicators model for volatility using intra-daily data. *Journal of Econometrics*, *131*, 3–27. [CrossRef]

Fan, J., & Wang, Y. (2007). *Multi-scale jump and volatility analysis for high-frequency financial data*. Available online: https://papers.ssrn.com/sol3/papers.cfm?abstract_id=957607 (accessed on 20 May 2025).

Gao, J., Peng, B., Wu, W. B., & Yan, Y. (2024). Time-varying multivariate causal processes. *Journal of Econometrics*, *240*, 105671. [CrossRef]

Ghosal, S., Ghosh, J. K., & van der Vaart, A. W. (2000). Convergence rates of posterior distributions. *Annals of Statistics*, *28*(2), 500–531. [CrossRef]

Huang, X., & Tauchen, G. T. (2005). The relative contribution of jumps to total price variance. *Journal of Financial Econometrics*, *3*(4), 456–499. [CrossRef]

Jacquier, E., Polson, N. G., & Rossi, P. E. (2004). Bayesian analysis of stochastic volatility models with fat-tails and correlated errors. *Journal of Econometrics*, *122*(1), 185–212. [CrossRef]

Kalli, M., & Griffin, J. E. (2014). Time-varying sparsity in dynamic regression models. *Journal of Econometrics*, *178*(2), 779–793. [CrossRef]

Kim, D., & Wang, Y. (2016). Unied discrete-time and continuous-time models and statistical inferences for merged low-frequency and high-frequency financial data. *Journal of Econometrics*, *194*(2), 220–230. [CrossRef]

Koop, G., & Korobilis, D. (2022). Bayesian dynamic variable selection in high dimensions. *International Economic Review*, *64*(3), 1047–1074. [CrossRef]

Opschoor, A., & Lucas, A. (2023). Time-Varying variance and skewness in realized volatility measures. *International Journal of Forecasting*, *39*, 827–840. [CrossRef]

Song, X., Kim, D., Yuan, H., Cui, X., Lu, Z., Zhou, Y., & Wang, Y. (2020). Volatility analysis with realized GARCH-Ito models. *Journal of Econometrics*, *222*(1), 393–410. [CrossRef]

Taspinar, S., DoGan, O., Chae, J., & Bera, A. K. (2021). Bayesian inference in spatial stochastic volatility models: An application to house price returns in Chicago. *Oxford Bulletin of Economics and Statistics*, *83*(5), 1243–1272. [CrossRef]

Todorov, V. (2009). Estimation of continuous-time stochastic volatility models with jumps using high-frequency data. *Journal of Econometrics*, *148*, 131–148. [CrossRef]